Discovery of CTSK$^+$ Periosteal Stem Cells Mediating Bone Repair in Orbital Reconstruction

Zeyang Liu,[1,2] Jin Liu,[1,2] Jipeng Li,[1,2] Yinwei Li,[1,2] Jing Sun,[1,2] Yuan Deng,[1,2] and Huifang Zhou[1,2]

[1]Department of Ophthalmology, Ninth People's Hospital, Shanghai Jiao Tong University School of Medicine, Shanghai, China
[2]Shanghai Key Laboratory of Orbital Diseases and Ocular Oncology, Shanghai, China

Correspondence: Huifang Zhou, Department of Ophthalmology, Ninth People's Hospital, Shanghai Jiao Tong University School of Medicine; 639 Zhizaoju Road, Shanghai, China; fangzzfang@sjtu.edu.cn.
Yuan Deng, Department of Ophthalmology, Ninth People's Hospital, Shanghai Jiao Tong University School of Medicine; 639 Zhizaoju Road, Shanghai, China; ophden@163.com.

ZL and JL contributed equally to the work presented here and should therefore be regarded as equivalent authors.

Received: December 29, 2022
Accepted: July 28, 2023
Published: August 28, 2023

Citation: Liu Z, Liu J, Li J, et al. Discovery of CTSK$^+$ periosteal stem cells mediating bone repair in orbital reconstruction. *Invest Ophthalmol Vis Sci.* 2023;64(11):30. https://doi.org/10.1167/iovs.64.11.30

Purpose. The purpose of this study was to explore the role of cathepsin K positive (CTSK$^+$) periosteal stem cells (PSCs) in orbital bone repair and to clarify the source of endogenous stem cells for orbital bone self-repair.

Methods. Periosteum samples obtained by clinical orbital bone repair surgery were analyzed, after which immunofluorescence and immunohistochemical staining were used to detect the content of bone marrow-derived cells and CTSK$^+$ PSCs in periosteum as well as the mobilization of PSCs. CTSK$^+$ PSCs were characterized by flow cytometry. Transcriptome sequencing was used to compare the transcriptomic characteristics of CTSK$^+$ PSCs and bone marrow mesenchymal stem cells (BMSCs).

Results. The orbital periosteum contained CTSK$^+$CD200$^+$ cell lineage, including CD200$^+$CD105$^-$ PSCs and CD200$^+$CD105$^+$ progenitor cells. CTSK and osteocalcin (OCN) colocalized in the inner layer of the orbital periosteum, suggesting the osteogenic differentiation potential of CTSK$^+$ PSCs. CTSK expression was much higher in periosteum after mobilization. Immunofluorescence showed low amounts of scattered CD31$^+$ and CD45$^+$ cells in the orbital periosteum. The stem cell characteristics of CTSK$^+$ PSCs were verified by multidirectional differentiation. Flow cytometry found CD200$^+$CD105$^-$ CTSK$^+$ PSCs and CD200^{variant}CD105$^+$ progenitor cells. Transcriptome sequencing of CTSK$^+$ PSCs and BMSCs found 3613 differential genes with significant differences. Gene Ontology (GO) analysis showed the differences between the two types of stem cells, revealing that PSCs were more suitable for intramembranous osteogenesis.

Conclusions. CTSK$^+$ PSCs may be endogenous stem cells for orbital bone repair. They are mobilized after orbital fracture and have unique features suitable for intramembranous osteogenesis, completely different from BMSCs.

Keywords: orbit, bone repair, cathepsin K (CTSK), periosteal stem cells (PSCs), bone marrow mesenchymal stem cells (BMSCs)

Severe orbital bone defects can cause blindness and seriously threaten patients' lives.[1] Patients with severe orbital bone defects (fracture has affected movement, function, or eye placement) usually require reconstructive surgery. Yet, this type of surgery may be challenging and associated with a high complication rate.[2] The main problem is that critical-sized bony defects do not have enough bony tissue to heal spontaneously.[3–5] One potential cause for inadequate bone repair is decreased or inadequate supply of osteogenic precursor cells. The location of these cells is unclear within the bony orbit. Thus, in-depth research on stem cells in orbital bone is of utmost importance.

Orbital bone has a unique anatomy and is mainly composed of thin cortical bone with a thickness of about 2 mm.[6] Although there is no bone marrow, this type of bone has a large specific surface area and abundant periosteum coverage, that is, great intramembranous osteogenic capability.[7,8] The source of stem cells for intramembranous osteogenesis has long been debated.[9–11] The classic theory suggests that stem cells in the periosteum are mainly bone marrow mesenchymal stem cells (BMSCs),[12–14] thus posing a great challenge to orbit self-repair.[5,15,16] Recent studies have found that the orbital bone can achieve a certain degree of self-repair after 4 to 6 months of conservative or surgical treatment in patients with orbital fractures,[17,18] suggesting the presence of in situ stem cells in the orbital periosteum. Yet, the exact source of orbital osteogenic precursor cells remains unclear.

The periosteum is a thin layer of connective tissue covering the surface of the bone.[19–21] It is composed of an outer fibrous layer and an inner germinal layer.[22] Periosteum is mainly responsible for the formation of the cortical bone.[23,24] The osteogenic ability mainly depends on the highly heterogeneous cells with multidirectional differentiation ability in the germinal layer.[25,26] Using lineage tracing technology, researchers found Nestin$^+$,[27] Sox9$^+$,[28,29]

Investigative Ophthalmology & Visual Science

Mx1+αSMA+,[30,31] and other osteogenic cell lineages in the periosteum. In 2015, Chan et al. identified skeletal stem cells and demonstrated them as the source of skeletal tissues,[32] which brought a new standing of skeletal tissue development and repair. Yet, whether there are periosteal stem cells (PSCs) of in situ origin in the periosteum remains unclear.

Cathepsin K (CTSK) is an osteoclast-specific protein mainly distributed in lysosomes that mediates tissue degradation.[33] Recent studies have demonstrated the osteogenic potential of CTSK+ cells.[34–36] Based on the discovery of CTSK+ cells in the metaphyseal cortex in 2013[37] and the discovery of skeletal stem cells in 2015,[32] Debnath et al. further revealed the developmental lineage and function of CTSK+ cell subsets,[38] finding that they are widely distributed on the surface of the periosteum of long bones and skulls. They confirmed that CTSK+ PSCs are intramembranous osteogenic stem cells. In addition, another study found that the deletion of tumor suppressor genes in CTSK+ cells could lead to the formation of subperiosteal osteosarcoma instead of other types of bone tumors in the metaphyseal growth plate,[38] which suggests that CTSK+ cells are important cells responsible for intramembranous osteogenesis.

In the present study, we used periosteum samples from orbital surgery to explore the function and cellular characteristics of CTSK+ PSCs in orbital bone repair. We compared the transcriptomic characteristics of CTSK+ PSCs and BMSCs, representing the difference between intramembranous osteogenic and endochondral osteogenic stem cells. The aim of this study was to clarify the real stem cell source of orbital bone repair apart from BMSCs in classic theory and explore the underlying mechanisms.

Materials and Methods

Histopathological Evaluation of Human Periosteum

Patients and Controls. Patients aged 18 to 65 years old who underwent orbital repair surgery (experimental group) or orbital decompression surgery (control group) and who were not using bone-related drugs, including glucocorticoids, over the past year were included in this study. Tissue from one patient was defined as one sample. The periosteum samples of the experimental group were taken from the bone fragments removed from the medial and lower orbital wall in orbital repair surgery of blow-out fracture; the periosteum samples of the control group were taken from the bone fragments removed from the medial and lower orbital wall in orbital decompression surgery (see the Table). The bone marrow samples were from the femoral fracture intramedullary nail internal fixation. The informed consent was obtained from each subject as approved by the ethics committee of Shanghai Ninth People's Hospital, Shanghai Jiao Tong University School of Medicine.

Histopathological Evaluation. The bone chips removed during the operation were rinsed three times with normal saline to remove residual blood or tissue residue. Samples were then placed in a 10% neutral formalin solution and fixed overnight. The fixed bone slices were decalcified with EDTA decalcification solution for at least 14 days, then dipped in wax, embedded, sectioned, and evaluated by immunofluorescence, immunohistochemistry, and hematoxylin and eosin (H&E) staining.

Characterization of CTSK+ PSCs

Cell Isolation and Culture. CTSK+ PSCs were isolated from the periosteum samples. Briefly, the periosteum samples were washed with PBS and then cut into small fragments (1 mm * 1 mm) and digested with collagenase A (2 mg/mL; Sigma-Aldrich) and dispase II (2 mg/mL; Gibco) overnight at 37°C with agitation at 200 rpm. Next, the suspension was centrifuged at 2000 rpm for 10 minutes, and the cell pellet was resuspended with complete culture medium (α-MEM supplemented with 10% fetal bovine serum (FBS) and 1% penicillin/streptomycin; Gibco). PSCs were rinsed after 24 hours to remove nonadherent cells and were then cultured for 7 days. Bone marrow stem cells were isolated from the bone marrow grinding samples. The complete culture medium mentioned above was added to the bone marrow samples. The samples were fully resuspended and filtrated through a 40 µm filter. The suspension was then seeded in a 10 cm culture dish and cultured for 24 hours. Next, the medium was changed, and cells were rinsed with PBS to remove nonadherent cells. PSCs and

Table. Clinical Annotation of Patients and Samples

	Experimental Group	Control Group
Individual samples number	9	8
Age	18–40 Y/O: 7 patients 41–65 Y/O: 2 patients	18–40 Y/O: 5 patients 41–65 Y/O: 3 patients
Gender	Male: 5 patients Female: 4 patients	Male: 3 patients Female: 5 patients
Time point of sample collection	5–10 days after injury: 7 patients 10–14 days after injury: 2 patients	During surgery
Fracture category	Orbit blow-out fracture Left: 4 patients Right: 3 patients Bilateral: 2 patients	Artificial bone defects in orbital decompression surgery Left: 1 patient Right: 1 patient Bilateral: 6 patients
Glucocorticoid use	No	No glucocorticoid use: 2 patients 1.0–3.0 y ago: 2 patients 3.1–5.0 y ago: 2 patients Over 5.0 y ago: 2 patients
Other bone-related drug use	No	No

BMSCs were passaged when the cells reached 80% to 90% confluency. Cells passaged three times were used for further experiments.

Cell Differentiation. A total of 3×10^5 PSCs were plated on each well of a 24-well plate. For in vitro osteogenic differentiation, PSCs were cultured in an osteogenic medium (complete culture medium with 50 mg/mL ascorbic acid, 100 nM dexamethasone, and 10 mM β-glycerophosphate) for 14 days and then subjected to Alizarin Red S (ARS) staining. For in vitro adipogenic differentiation, PSCs were cultured in an adipogenic medium (Stem Cell Technologies) for 14 days and then subjected to Oli Red staining. For in vitro chondrogenic staining, 2×10^6 PSCs were added into a centrifuge tube and then centrifuged. The cell pellet was cultured in a chondrogenic medium (Stem Cell Technologies) for 14 days and then subjected to Alcian Blue staining.

Flow Cytometry. The PSCs passaged 3 times were digested with trypsin and EDTA and centrifuged at 800 rpm for 4 minutes. PSCs were resuspended with 100 µL of sheath fluid. Then, the corresponding antibody was added according to the required concentration of the antibody specification and incubated on ice for 30 minutes in the dark. Each group of detection indicators required setting up a group of single dye tubes and a group of isotype control tubes, which were used to avoid nonspecific staining and assist in gating. The cells in each tube were centrifuged at 800 rpm for 4 minutes to discard the antibody and then washed with sheath fluid 3 times. The cells were resuspended with 500 µL of fresh sheath fluid and then tested on the machine for identification. All samples were tested for at least three times.

RNA Sequencing

The extracted primary CTSK+ PSCs and primary BMSCs were cultured in vitro for three passages, after which RNA sequencing was conducted. Briefly, total RNA was extracted by TRIzol solution. After quality control, mRNA was purified with magnetic beads and fragmented into oligonucleotides. Next, the gene library was created and sequenced on the Illumina platform. The sequencing data were analyzed by bioinformatics to analyze the reads of each corresponding gene. Genes with a difference of $|\log2 \text{ fold change}| \geq 1$ and P value < 0.05 were defined as genes with a significant difference. Then, Gene Ontology (GO) analysis, Kyoto Encyclopedia of Genes and Genomes (KEGG) enrichment analysis, and other advanced analysis were conducted.

Statistical Analysis

All experiments were performed independently and repeated at least three times based on the number of

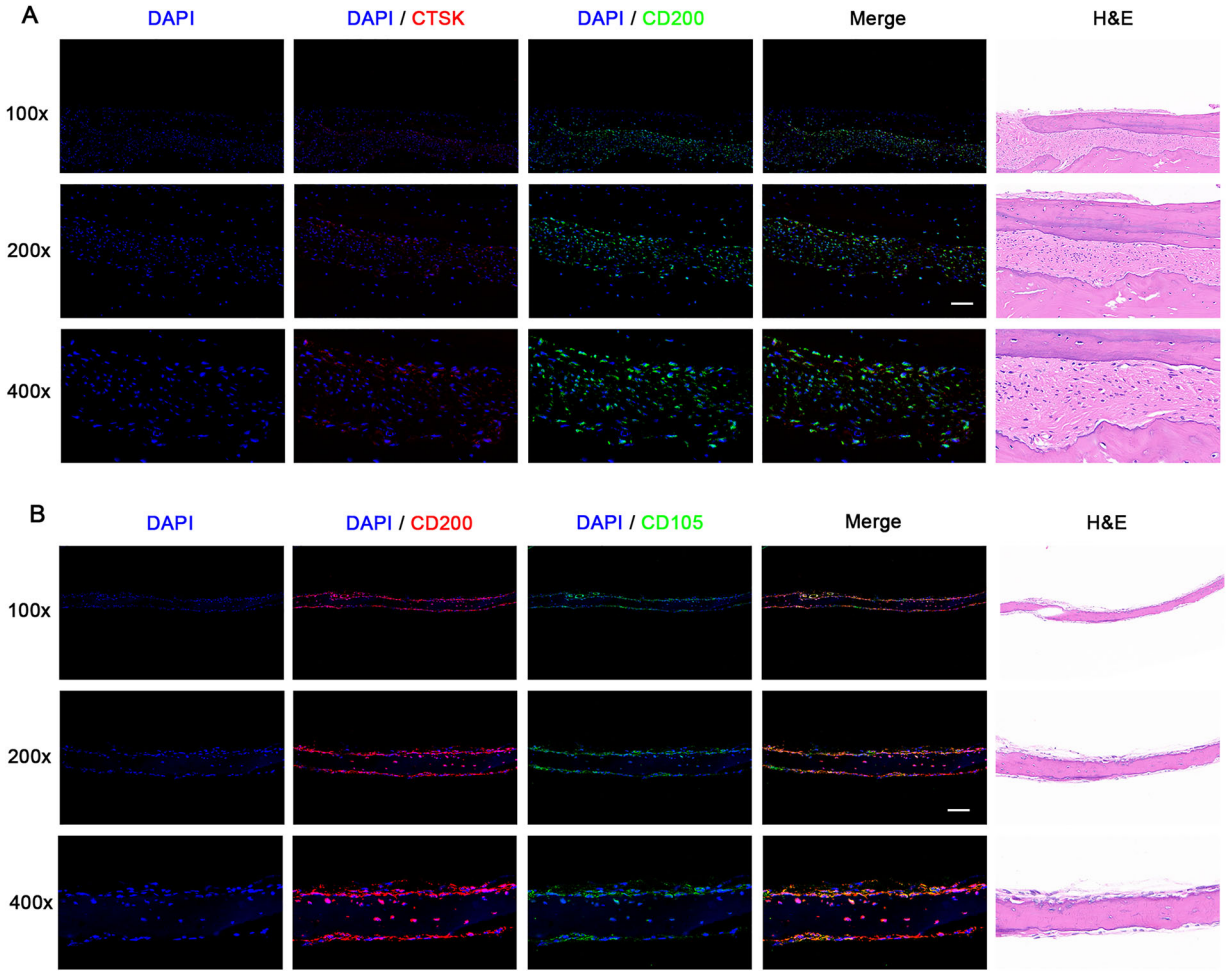

Figure 1. Distribution of CTSK+PSCs in human orbital periosteum. CTSK+CD200+ (**A**), CD200+CD105−, and CD200variantCD105+ cells (**B**) distributed in the inner layer of the orbital periosteum. Nine specimens ($n = 9$) were stained with CTSK/CD200 and 6 displayed similar results as above (6/9 positive). Nine specimens ($n = 9$) were stained with CD200/CD105 and 7 displayed similar results as above (7/9 positive). Scale bar = 50 µm.

Investigative Ophthalmology & Visual Science

samples. All data were expressed as mean ± standard deviation. The *t*-test was used to analyze the statistical difference, and a P value < 0.05 represented a statistically significant difference (* represents $P < 0.05$ versus control; ** represents $P < 0.01$ versus control; and *** represents $P < 0.001$ versus control).

Results

Distribution of CTSK+ PSCs in Human Orbital Periosteum

To determine whether the orbital tissue contains CTSK+ PSCs, we collected bone fragments with periosteum samples taken about 7 days after the fracture, when the stem cells and precursor cells in the periosteum were fully mobilized. Two groups of highly specific labeling strategies were used to label CTSK+ PSCs and progenitors, that is, CTSK/CD200 to define the CTSK+ PSCs lineage and CD200/CD105 to distinguish PSCs and progenitors. As shown in Figure 1A, CTSK+CD200+ periosteal cells were evident in the periosteal specimens and mainly distributed in the inner surface of the orbital periosteum, close to a layer of bone, that is, the inner cell layer of the periosteum. Meanwhile, the periosteum contained both CD200+/CD105− and CD200variant/CD105+ cells (Fig. 1B).

CTSK+ PSCs Are Bone-Lineage Cells

Next, we examined the co-expression pattern of CTSK+ cells and osteocalcin (OCN). Co-labeled cells were found on the inner surface of the periosteum (Fig. 2A), suggesting that the CTSK+ cells are an osteogenic lineage. The results above were verified by immunohistochemical experiments (Fig. 2B).

Bone Marrow-Derived Cells May Only Partially Contribute to the Orbital Repair

The classical theory holds that the orbital bone lacks blood supply and does not contain bone marrow. We tested 4 markers: CD29, CD31 (a specific marker of vascular endothelial cells), CD34, and CD45 (common leukocyte antigen expressing on leukocytes in the bone marrow and cancellous bone). Our results showed low amounts of scattered CD31+ and CD45+ cells in the periosteal tissue (Figs. 3A–D), indicating that the orbital periosteum lacks bone marrow and blood supply and is a relatively isolated microenvironment.

CTSK+ PSCs Are Mobilized in Orbital Repair

The mobilization and expansion of stem cells during tissue damage are two of their most important characteristics. To confirm the stem cell properties of CTSK+ PSCs, we selected two different sources of periosteal tissue: (1) orbital bone and periosteum fragments derived from orbital decompression surgery, in which CTSK+ PSCs were still resting; (2) orbital bone and periosteum fragments derived from orbital repair surgery about 7 days after orbital fracture. CTSK+ PSCs have been fully activated at this time in large quantities. The results showed many CD200+CD105− PSCs and CD200variantCD105+ progenitor cells in the bone

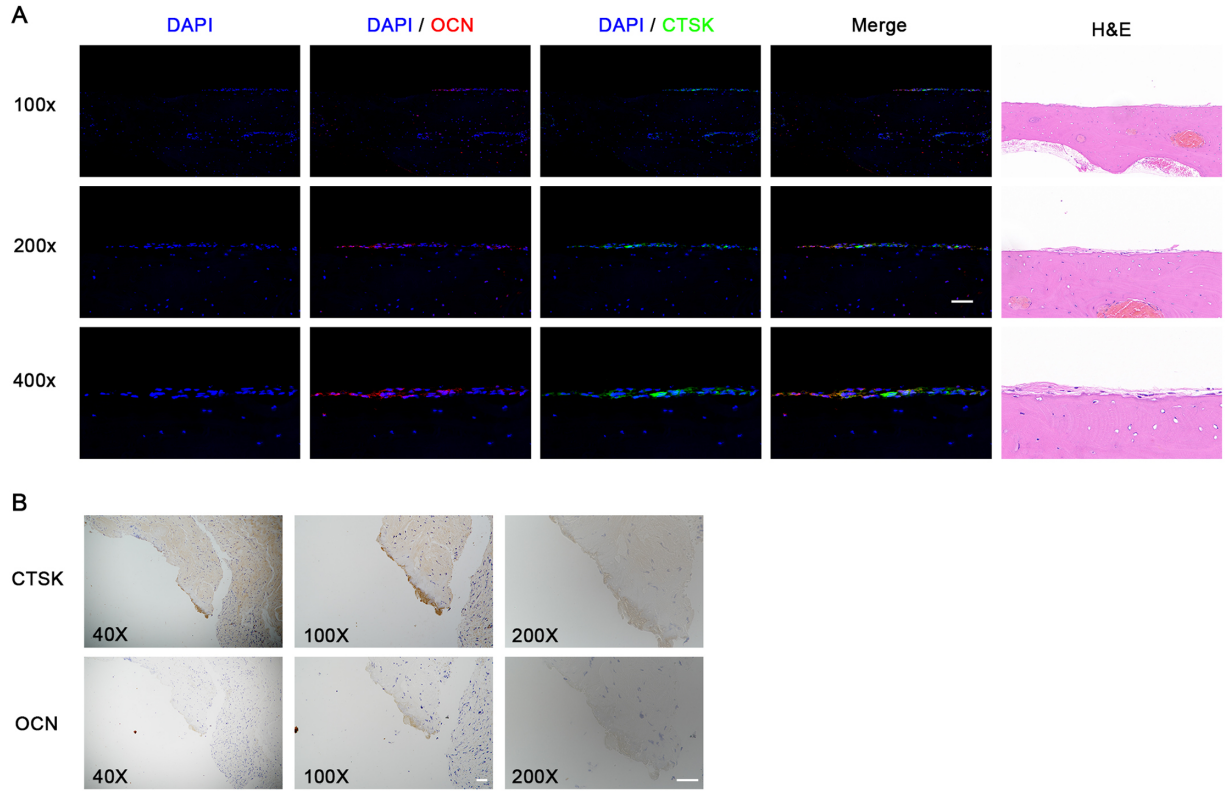

Figure 2. Expression of osteogenic markers in CTSK+ lineage. CTSK+ and OCN+ cells detected by IF (**A**) and immunohistochemical (IHC) (**B**) in the human orbital periosteum. CTSK and OCN were colocalized. Nine specimens ($n = 9$) were stained by immunofluorescence (IF) and six displayed similar results as above (6/9 positive). Scale bar = 50 µm.

Investigative Ophthalmology & Visual Science

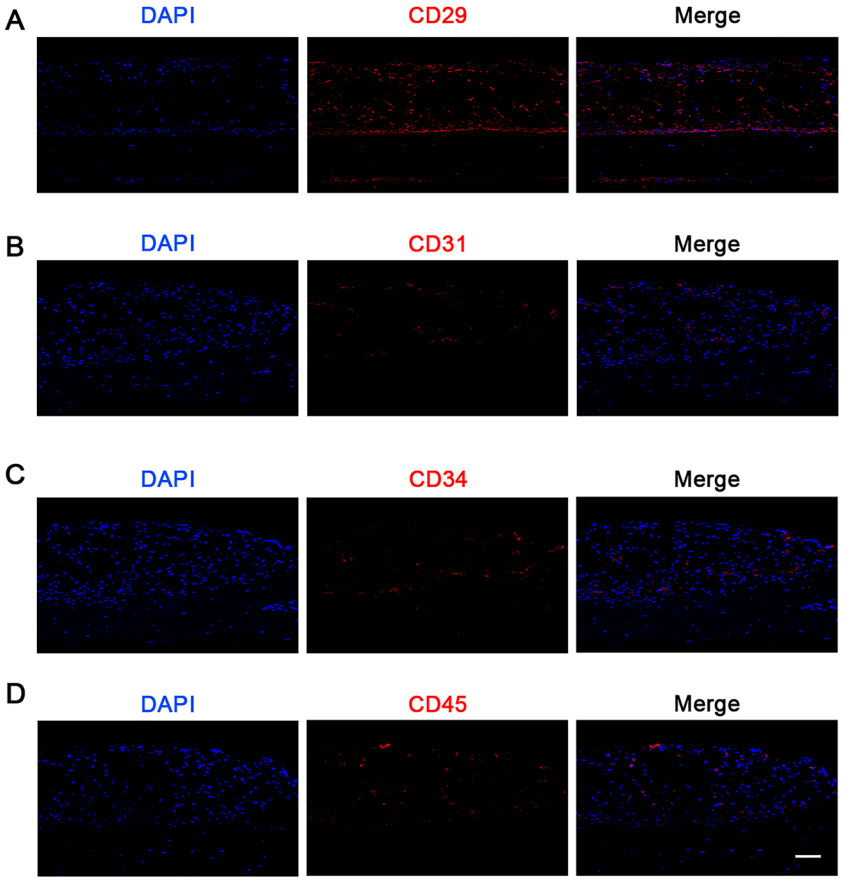

Figure 3. Expression of bone marrow and vascular related cell markers in orbital bone periosteum. $CD29^+$ (**A**) and $CD34^+$ (**C**) cells were positive, whereas low amount of scattered $CD31^+$ (**B**) and $CD45^+$ (**D**) cells were found in the human orbital bone periosteum. Seventeen specimens ($n = 17$) were stained and the number of samples displayed similar results as above was 13 for CD29 (13/17), 15 for CD31 (15/17), 12 for CD34 (12/17), and 16 for CD45 (16/17). Scale bar = 50 µm.

fragments derived from orbital repair, and the high fluorescence intensity (Fig. 4A). However, only a small population of $CD200^+CD105^-$ PSCs and $CD200^{variant}CD105^+$ progenitor cells with low fluorescence intensity (Fig. 4B) were detected in the bone fragments derived from orbital decompression. The statistical analysis of the positive rate of $CD200^+CD105^-$, $CD200^+CD105^+$, and $CD200^-CD105^+$ cells proved the difference (Figs. 4C–E). The above results suggest a promising stem cell property of PSCs. This result also suggests that $CTSK^+$ PSCs may have an important role in orbital bone repair.

Characterization of $CTSK^+$ PSCs

Next, we performed cell biological characterization of $CTSK^+$ PSCs. We collected orbital bone samples from orbital repair surgery. As shown in Figure 5, the orbital bone is a thin layer of cortical bone with certain light transmittance, whereas the periosteum is an extremely thin layer of fibrous membrane attached to the surface of the orbital bone (see Fig. 5A), rich in collagen fibers, with low cell content. Cells were mainly distributed on the junction surface of the periosteum and orbital bone (see Fig. 5D).

Subsequently, we isolated primary periosteal cells from the orbital periosteum. To determine the exact composition of isolated periosteal cells, we used flow cytometry to characterize the surface markers of periosteal cells (see Figs. 5E–L). The results showed that 80.73% of the cells were $CD200^+$ whereas 29.89% of the cells were $CD105^+$, which was in line with our definition of $CTSK^+$ PSCs and progenitors mentioned above, indicating that most of the extracted periosteal cells were $CTSK^+$ PSCs and progenitors. At the same time, we found no positive expression of CD31, CD34, and CD45. This result further confirmed the results in Figures 3 and 4. Under the light microscope, the $CTSK^+$ PSCs appeared with a long spindle shape (see Fig. 5B), a typical mesoderm-derived cell morphology. This is consistent with the results reported in previous studies, and it suggests that $CTSK^+$ PSCs belong to a subpopulation of mesenchymal stem cells (MSCs). The multidirectional differentiation results further showed that $CTSK^+$ PSCs could exert osteogenic, adipogenic, and chondrogenic differentiation (see Fig. 5C), proposing that they have mesodermal capabilities. The $CTSK^+$ cells isolated from orbital bone periosteum appear to have multipotency relative to mesodermal cell fates.

RNA Sequencing of $CTSK^+$ PSCs and BMSCs

BMSCs have been regarded as the pivotal stem cell in orbital bone repair according to the classical hypothesis for a long time. We suggest a potential bone regenerative role of $CTSK^+$ cells similar to those described by Debnath et al.[38] The difference in transcriptomic characteristics between these

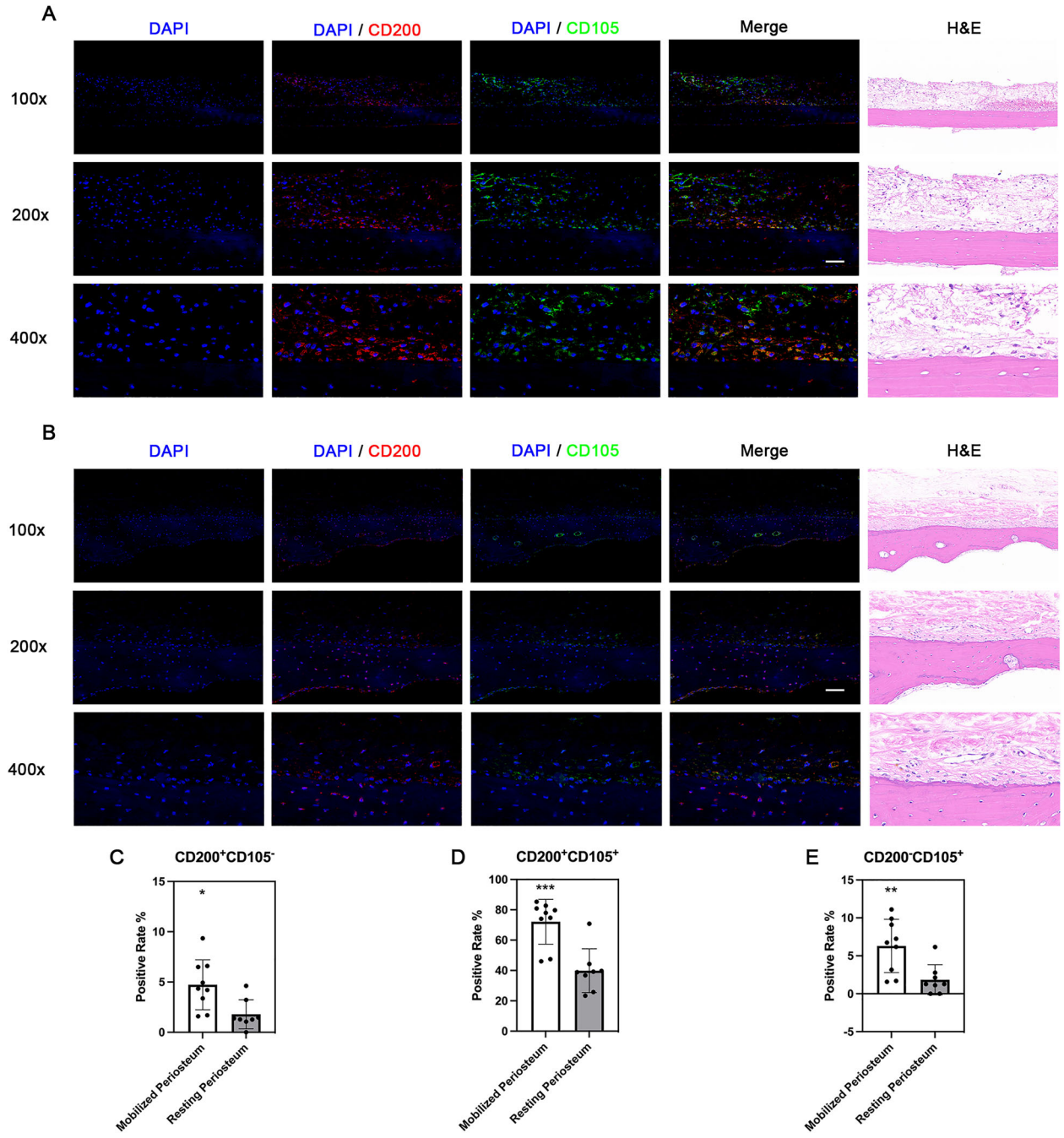

Figure 4. Distribution of CTSK$^+$PSCs in resting and mobilized periosteum. (**A**) CD200 and CD105 showed a high expression in the mobilized periosteum. Nine specimens ($n = 9$) were stained and seven displayed similar results as above (7/9). (**B**) CD200 and CD105 expression were low in the resting periosteum. Eight specimens ($n = 8$) were stained and seven displayed similar results as above (7/8). (**C-E**) The positive rate of (**C**) CD200$^+$CD105$^-$, (**D**) CD200$^+$CD105$^+$, and (**E**) CD200$^-$CD105$^+$ cells in the mobilized and resting periosteum under 400 times magnification. The *t*-test was used to analyze the statistical difference, and a *P* value < 0.05 represented a statistically significant difference (* represents $P < 0.05$ versus control; ** represents $P < 0.01$ versus control; and *** represents $P < 0.001$ versus control). Scale bar = 50 µm.

two types of stem cells needs to be further explored. In this study, we extracted CTSK$^+$ PSCs and BMSCs for transcriptomic analysis, finding that 14,545 genes were detected, including 3613 differential genes (1542 genes were upregulated in CTSK$^+$ PSCs, whereas 2071 genes were downregulated; Figs. 6A, 6B), indicating significant differences between the two cells. Then, we analyzed the different feature genes of PSCs and BMSCs according to the work of Debnath et al.[38] and found similar transcriptional features between human derived and mouse derived PSCs (Fig. 6C), indicating the cells we isolated truly represent a PSC-like population.

Subsequently, we performed GO enrichment analysis on the genes with significant differences. The results showed that the differential genes of the two types of stem cells were widely distributed in various gene categories (Fig. 6D),

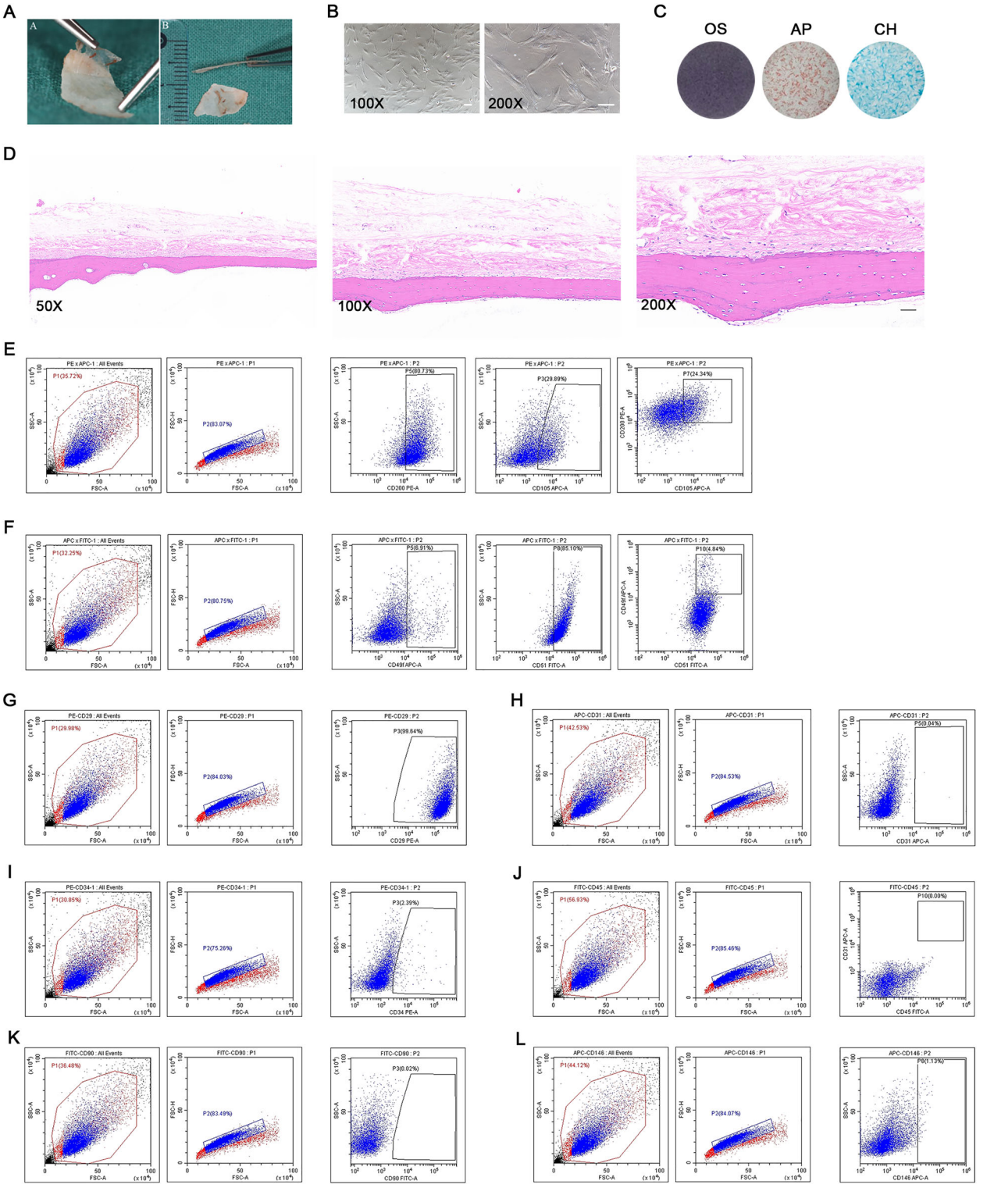

Figure 5. Characterization of periosteum tissue and CTSK+PSCs. (**A**) Bone fragments and periosteum obtained from orbital repair surgery. (**B**) Morphological observation of CTSK+ PSCs with typical MSC morphology. (**C**) Alizarin Red, Oil Red, and Alcian Blue Staining of CTSK+ PSCs. (**D**) H&E staining of orbital periosteum (from the same sample with Fig. 4B). (**E**) Flow cytometric characterization and gating strategy of CTSK+ PSCs including CD200/CD105, (F) CD49f/CD51, (G) CD29, (H) CD31, (I) CD34, (J) CD45, (K) CD90, and (L) CD146. Scale bar = 50 µm.

Investigative Ophthalmology & Visual Science

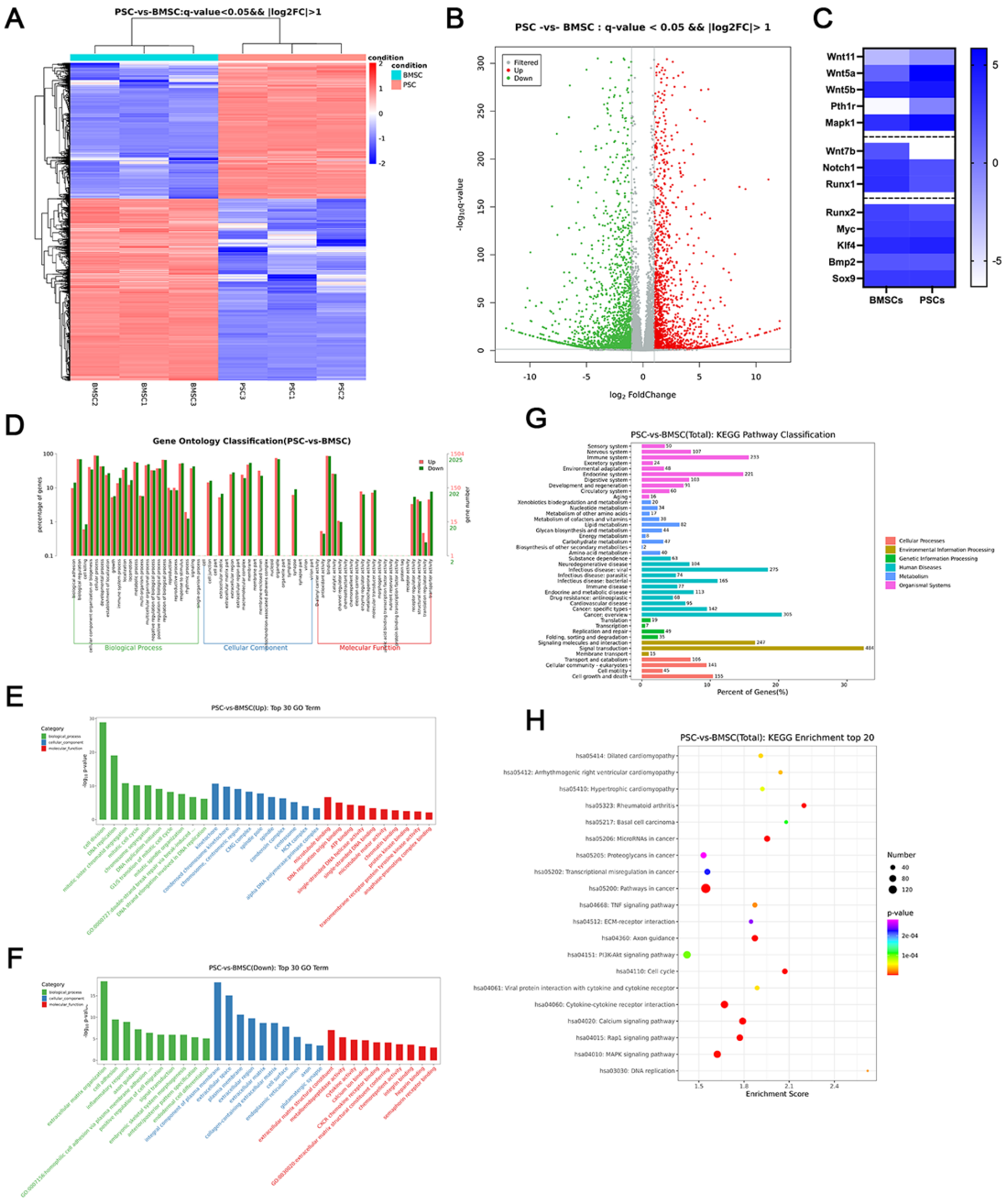

Figure 6. Transcriptomic analysis of CTSK+PSCs and BMSCs. (**A**) Gene expression heat map showing the number and distribution of differential genes between CTSK+PSCs and BMSCs. (**B**) Gene expression volcano plot showing the distribution of differential genes and the actual degree of difference. (**C**) Heatmap of gene expression in PSCs and non-CTSK BMSCs. (**D**) Overall GO enrichment analysis of differential genes. (**E**) GO functional clustering of upregulated genes in CTSK+ PSCs. (**F**) GO functional clustering of downregulated genes in CTSK+ PSCs. (**G**) Overall KEGG enrichment analysis of differential genes. (**H**) Bubble plot showing KEGG pathway enrichment of differential genes.

indicating that the two types of cells have different functions. CTSK+ PSCs' upregulated genes were mainly clustered in cell division, DNA replication, and cytoskeleton reorganization (Fig. 6E), indicating a stronger proliferation capability and more simple function. Among the genes upregulated in BMSCs, the functional clustering mainly included extracellular matrix remodeling, immune regulation, and cytoskeleton regulation. At the same time, functional clustering also detected the activation of multiple functions, such as cell signaling, cytokine secretion, cell adhesion, and chemokine receptor expression in BMSCs (Fig. 6F), indicating the more complex cell function of BMSCs.

We also performed KEGG pathway enrichment analysis on the differential genes. Our results showed that the differential genes were mainly enriched in signal transduction pathways and tumor-related pathways (Figs. 6G, 6H). Enriching tumor-related pathways mainly reflects cell proliferation activity, which may be related to the higher proliferation activity of CTSK+ PSCs. The enrichment of other pathways included cytokine-related pathways, calcium

ion-related pathways, Rap1 signaling pathway, MAPK signaling pathway, etc. Combined with the above GO functional enrichment results, these activated signaling pathways may be related to the complex biological functions of BMSCs. This part revealed the significant difference between intramembranous and endochondral osteogenic stem cells.

Discussion

The source of endogenous stem cells for orbital bone repair has always posed a challenging issue in orbital surgery.[9–11] The classical theory suggests that the orbital bone lacks endogenous stem cells in situ because the orbital bone is generally a thin cortical bone with no bone marrow.[5] The source of stem cells for orbital bone regeneration mainly depends on the extremely small amount of BMSCs.[12–14] In this study, we found abundant CTSK+ PSCs in the orbital periosteum (see Fig. 1). CTSK+ PSCs showed good osteogenic differentiation ability (see Fig. 2) that could mobilize and activate during orbital injury (see Fig. 4). A multidirectional differentiation ability was also detected (see Fig. 5), which was in line with the mesodermal capabilities. Moreover, the transcriptomic analysis suggested that CTSK+ PSCs have completely different transcriptomic characteristics and cellular functions from BMSCs (see Fig. 6). In addition, CTSK+ PSCs had features more suitable for intramembranous osteogenesis. This study sheds new light on the classical theory of the origin of endogenous stem cells for orbital bone repair (see Fig. 7).

Bones in different locations undergo different development and repair processes. Craniofacial bones are thinner and non-stress flat, unlike long bones.[6] This characteristic gives them a larger specific surface area and more periosteum, which is of great importance in intramembranous osteogenesis.[7,8] It also causes differences between the osteogenesis process of flat and long bones. These two unique osteogenesis processes mainly rely on the different biological behaviors of stem cells based on different cell types and their respective niches. CTSK+ PSCs and BMSCs can be found in different stem cell niches.[39,40] The discrepancy in their microenvironment and cell interactions determines their functional differences. Transcriptomic analysis revealed that CTSK+ PSCs had stronger proliferation activity, and their cell functions were less diverse (see Fig. 6), which matches the microenvironment of periosteum. The structure and composition of the periosteum are relatively simple.[19–21] They are mainly composed of fibrous connective tissue membranes, blood vessels, fibroblasts, and PSCs colonized within, not containing other complex types of cells.[22] The main function of the periosteum is to maintain cortical bone homeostasis and supply cortical bone nutrition.[23,24] When a bone defect occurs, the precursor cells in the periosteum divide, migrate, and undergo osteogenic differentiation.[41–43] This also indicates that CTSK+ PSCs are more in line with the cell characteristics required for intramembranous osteogenesis.

The function of BMSCs is more complex (see Fig. 6), presumably due to the complex bone marrow microenvironment.[44] The structure and composition of bone marrow include hematopoietic stem cells, stromal cells, and many immune cells in different states.[45] BMSCs need to maintain bone homeostasis through the continuous endochondral osteogenesis process[46,47] and take into account the maintenance of the hematopoietic stem cell microenvironment.[48] Besides, the immune homeostasis of bone marrow also depends on BMSCs.[49] Thus, their functions are more complex, with many upregulated gene properties, including cell interaction, immune regulation, and similar. The complexity of functionally enriched gene types of BMSCs is also in line with their roles and characteristics in the bone marrow.

We suggest that the CTSK+ precursor cells might have an important role in the repair of orbital bone defects. However, the study still has also some limitations. First, stem cell characteristics of PSCs were limited to in vitro experiments, and in-depth verification of orbital bone in situ tissue engineering repair experiments is still required. Second, the characteristics of PSCs were only assessed using transcriptome sequencing analysis. It is still necessary to clarify the source, developmental lineage, and fate decision of PSCs through lineage tracing technology and search for critical genes in the process of proliferation and differentiation. Meanwhile, the PSCs and BMSCs used for RNA sequencing did not undergo fluorescent activated cell sorting (FACS) sorting. The residual hematopoietic cells or macrophages may interfere the transcriptional features of these two cell types and further experiment with more accuracy is still needed. In addition, exploring the critical functional genes of PSCs is of

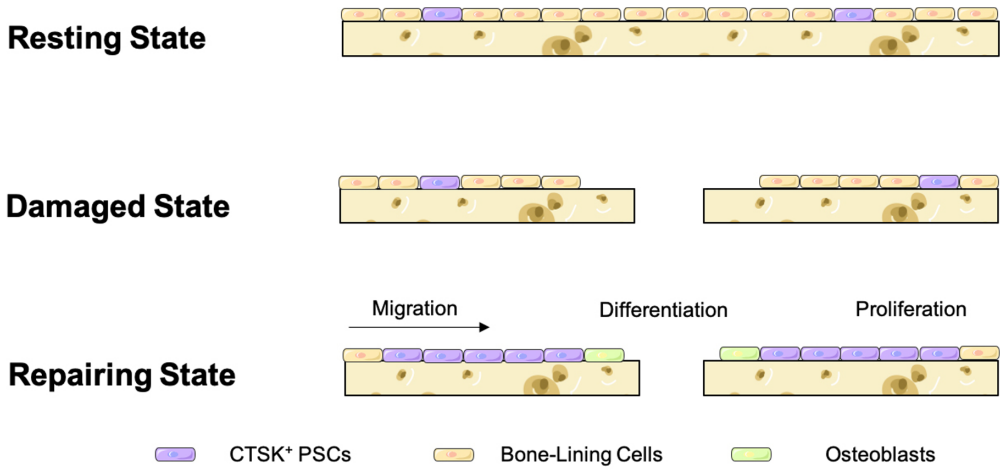

Figure 7. Schematic illustration of CTSK+ PSCs-mediated orbital bone repair.

great importance for their clinical application and transformation. We can use genetic engineering or stem cell technology to activate PSCs in situ, which can help to achieve in situ repair of orbital bone defects without surgery. Furthermore, conducting in-depth orbital periosteum research is a promising research direction. As a critical component of the orbital microenvironment, the orbital periosteum has a crucial role in orbital bone development and repair. It is well worth exploring the pathophysiological role of the periosteum in the process of various orbital diseases, as this could further our understanding of the pathogenic mechanism related to orbital periosteum and provide a more comprehensive panorama display of orbital diseases, thereby contributing to developing novel more effective therapies.

Conclusions

The endogenous stem cells for orbital bone repair may be the CTSK+ PSCs. They are osteogenic and mobilized after an orbital fracture. In addition, these cells have higher proliferation activity and less diverse cell functions from BMSCs, which are suitable for intramembranous osteogenesis.

Acknowledgments

Supported by the National Natural Science Foundation of China (82071003, 82271122, and 82203890) and the Shanghai Sailing Program (22YF1421500).

Disclosure: **Z. Liu**, None; **J. Liu**, None; **J. Li**, None; **Y. Li**, None; **J. Sun**, None; **Y. Deng**, None; **H. Zhou**, None

References

1. Song X, Li L, Sun Y, et al. Long-term infectious complications of using porous polyethylene mesh for orbital fracture reconstruction. *Medicine*. 2016;95:e3819.
2. Qian Z, Zhuang A, Lin M, et al. Treatment of orbital blowout fracture using porous polyethylene with embedded titanium. *J Craniofac Surg*. 2015;26(2):569–572.
3. Potter JK, Malmquist M, Ellis E. Biomaterials for reconstruction of the internal orbit. *Oral Maxillofac Surg*. 2012;24:609–627.
4. Dubois L, Steenen SA, Gooris PJ, Bos RR, Becking AG. Controversies in orbital reconstruction-III. Biomaterials for orbital reconstruction: a review with clinical recommendations. *Int J Oral Maxillofac Surg*. 2016;45(1):41–50.
5. Unsold R. Computed tomographic anatomy of the orbit. *Int Ophthalmol Clin*. 1982;22(4):45–80.
6. Gentry LR. Anatomy of the orbit. *Neuroimaging Clin N Am*. 1998;8(1):171–194.
7. Long F. Building strong bones: molecular regulation of the osteoblast lineage. *Nat Rev Mol Cell Biol*. 2011;13(1):27–38.
8. Feehan J, Nurgali K, Apostolopoulos V, et al. Circulating osteogenic precursor cells: building bone from blood. *EBioMedicine*. 2019;39:603–611.
9. Marx RE. Bone and bone graft healing. *Oral Maxillofac Surg Clin North Am*. 2007;19(4):455–466.
10. Oftadeh R, Perez-Viloria M, Villa-Camacho JC, et al. Biomechanics and mechanobiology of trabecular bone: a review. *J Biomech Eng*. 2015;137(1):0108021–01080215.
11. Franz-Odendaal TA. Induction and patterning of intramembranous bone. *Front Biosci (Landmark Ed)*. 2011;16:2734–2746.
12. Chen CT, Chen YR. Update on orbital reconstruction. *Curr Opin Otolaryngol Head Neck Surg*. 2010;18(4):311–316.
13. Joshi S, Kassira W, Thaller SR. Overview of pediatric orbital fractures. *J Craniofac Surg*. 2011;22(4):1330–1332.
14. Iatrou I, Theologie-Lygidakis N, Angelopoulos A. Use of membrane and bone grafts in the reconstruction of orbital fractures. *Oral Surg Oral Med Oral Pathol Oral Radiol Endod*. 2001;91(3):281–286.
15. Hayreh SS. Orbital vascular anatomy. *Eye (Lond)*. 2006;20(10):1130–1144.
16. So WK, Cheung TH. Molecular regulation of cellular quiescence: a perspective from adult stem cells and its niches. *Methods Mol Biol*. 2018;1686:1–25.
17. Young SM, Kim YD, Kim SW, et al. Conservatively treated orbital blowout fractures: spontaneous radiologic improvement. *Ophthalmology*. 2018;125:938–944.
18. Zhao LP, Sun J, Li ZK, et al. Bioresorbable implants in reduction of paediatric zygomaticomaxillary complex fractures concurrent with internal orbital reconstruction. *J Craniofac Surg*. 2022 (Online ahead of print).
19. Sharma P, Williams R, Monaghan A. Spontaneous mandibular regeneration: another option for mandibular reconstruction in children. *Br J Oral Maxillofac Surg*. 2013;51(5):e63–e66.
20. Kojimoto H, Yasui N, Goto T, et al. Bone lengthening in rabbits by callus distraction. The role of periosteum and endosteum. *J Bone Joint Surg Br*. 1988;70(4):543–549.
21. Huang RL, Tremp M, Ho CK, et al. Prefabrication of a functional bone graft with a pedicled periosteal flap as an in vivo bioreactor. *Sci Rep*. 2017;7(1):18038.
22. Nahian A, Chauhan PR. Histology, periosteum and endosteum. In: *StatPearls*. Treasure Island, FL: StatPearls Publishing; 2021.
23. Pazzaglia UE, Reguzzoni M, Casati L, et al. Long bone human anlage longitudinal and circumferential growth in the fetal period and comparison with the growth plate cartilage of the postnatal age. *Microsc Res Tech*. 2019;82(3):190–198.
24. Kohara Y, Soeta S, Izu Y, et al. Distribution of type VI collagen in association with osteoblast lineages in the groove of ranvier during rat postnatal development. *Ann Anat*. 2016;208:58–68.
25. Bolander J, Ji W, Geris L, et al. The combined mechanism of bone morphogenetic protein- and calcium phosphate induced skeletal tissue formation by human periosteum derived cells. *Eur Cell Mater*. 2016;31:11–25.
26. Groeneveldt LC, Herpelinck T, Maréchal M, et al. The bone-forming properties of periosteum-derived cells differ between harvest sites. *Front Cell Dev Biol*. 2020;8:554984.
27. Tournaire G, Stegen S, Giacomini G, et al. Nestin-GFP transgene labels skeletal progenitors in the periosteum. *Bone*. 2020;133:115259.
28. He X, Bougioukli S, Ortega B, et al. Sox9 positive periosteal cells in fracture repair of the adult mammalian long bone. *Bone*. 2017;103:12–19.
29. Kuwahara ST, Serowoky MA, Vakhshori V, et al. Sox9+ messenger cells orchestrate large-scale skeletal regeneration in the mammalian rib. *Elife*. 2019;8:e40715.
30. Matthews BG, Grcevic D, Wang L, et al. Analysis of αSMA-labeled progenitor cell commitment identifies notch signaling as an important pathway in fracture healing. *J Bone Miner Res*. 2014;29(5):1283–1294.
31. Ortinau LC, Wang H, Lei K, et al. Identification of functionally distinct Mx1+αSMA+ periosteal skeletal stem cells. *Cell Stem Cell*. 2019;25(6):784–796.
32. Chan CKF, Eun YS, James YC, et al. Identification and specification of the mouse skeletal stem cell. *Cell*. 2015;160(1-2):285–298.
33. Dodds RA, Connor JR, Drake F, et al. Cathepsin K mRNA detection is restricted to osteoclasts during fetal mouse development. *J Bone Miner Res*. 1998;13:673–682.

Investigative Ophthalmology & Visual Science

34. Kyung SK, Jung MH, Daniel JH, et al. Induction of Lrp5 HBM-causing mutations in Cathepsin-K expressing cells alters bone metabolism. *Bone*. 2019;120:166–175.
35. Nicolas B, Julia B, Jean CR, et al. Cathepsin K controls cortical bone formation by degrading periostin. *J Bone Miner Res*. 2017;32(7):1432–1441.
36. Ding Y, Mo C, Geng J, et al. Identification of periosteal osteogenic progenitors in jawbone. *J Dent Res*. 2022;220345221084200.
37. Yang WT, Wang JG, Douglas CM, et al. Ptpn11 deletion in a novel progenitor causes metachondromatosis by inducing hedgehog signalling. *Nature*. 2013;499(7459):491–495.
38. Debnath S, Yallowitz AR, McCormick J, et al. Discovery of a periosteal stem cell mediating intramembranous bone formation. *Nature*. 2018;562:133–139.
39. Han YJ, Feng H, Sun J, et al. Lkb1 deletion in periosteal mesenchymal progenitors induces osteogenic tumors through mTORC1 activation. *J Clin Invest*. 2019;129(5):1895–1909.
40. Duchamp de Lageneste O, Julien A, Abou-Khalil R, et al. Periosteum contains skeletal stem cells with high bone regenerative potential controlled by periostin. *Nat Commun*. 2018;9(1):773.
41. Kegelman CD, Nijsure MP, Moharrer Y, et al. YAP and TAZ promote periosteal osteoblast precursor expansion and differentiation for fracture repair. *J Bone Miner Res*. 2021;36(1):143–157.
42. Percival CJ, Richtsmeier JT. Angiogenesis and intramembranous osteogenesis. *Dev Dyn*. 2013;242(8):909–922.
43. Ryan C, Thomas LC. Bone cell bioenergetics and skeletal energy homeostasis. *Physiol Rev*. 2017;97:667–698.
44. Baker N, Boyette LB, Tuan RS. Characterization of bone marrow-derived mesenchymal stem cells in aging. *Bone*. 2015;70:37–47.
45. Ankit S, Harsh N, Benjamin L, et al. Mechanisms of bone development and repair. *Nat Rev Mol Cell Biol*. 2020;21(11):696–711.
46. Lin H, Sohn J, Shen H, Langhans MT, Tuan RS. Bone marrow mesenchymal stem cells: aging and tissue engineering applications to enhance bone healing. *Biomaterials*. 2019;203:96–110.
47. Charbord P. Bone marrow mesenchymal stem cells: historical overview and concepts. *Hum Gene Ther*. 2010;21(9):1045–56.
48. Ding DC, Shyu WC, Lin SZ. Mesenchymal stem cells. *Cell Transplant*. 2011;20(1):5–14.
49. Shen B, Alpaslan T, Jessalyn MU, et al. A mechanosensitive peri-arteriolar niche for osteogenesis and lymphopoiesis. *Nature*. 2021;591(7850):438–444.

Investigative Ophthalmology & Visual Science